

Non-isothermal crystallization kinetics of polypropylene/poly(lactic acid)/maleic anhydride-grafted polypropylene blends

Zhi-fei Bai¹ · Qiang Dou¹

Received: 31 October 2015 / Accepted: 14 May 2016 / Published online: 27 May 2016
© Akadémiai Kiadó, Budapest, Hungary 2016

Abstract The non-isothermal crystallization kinetics of neat polypropylene (PP), PP/poly(lactic acid) (PLA) blend and PP/PLA/maleic anhydride-grafted polypropylene (MAH-g-PP) blend were investigated by means of differential scanning calorimetry. Jeziorny's and Mo's models were employed to analyze the non-isothermal crystallization kinetics. The nucleation parameters (K_g) and activation energies (ΔE) of non-isothermal crystallization were calculated by the modified Lauritzen–Hoffman equation and Kissinger's equation, respectively. The results show that Jeziorny's and Mo's models are suitable for describing the non-isothermal crystallization kinetics of the samples. PP/PLA (80/20) blend shows the fastest crystallization rate due to the nucleation effect of the dispersed PLA particles in PP matrix. However, the crystallization of PP in the blend is restricted by the incorporation of the MAH-g-PP. The K_g and ΔE are in the order: PP/PLA/MAH-g-PP (64/20/16) blend > neat PP > PP/PLA (80/20) blend.

Keywords Polypropylene · Poly(lactic acid) · Maleic anhydride-grafted polypropylene · Blend · Non-isothermal crystallization kinetics

Introduction

Petroleum-based polymers have been developed at least a hundred years, and they have been used in many fields ranging from industry and agriculture to commodity goods,

which play an important role in the improvement of the quality of human life [1–4]. These polymers are produced from crude oil or fossil fuel and end up as nondegradable waste after their service time. Landfill and incineration are two main methods of disposing polymer waste, while they are not free from environmental pollution problems [5, 6]. Therefore, much attention has been focused on developing environmentally friendly polymers with biodegradable properties. Biodegradable polymers can decompose by microbes in natural environment and easily convert to carbon dioxide and water [7]. From the ecological viewpoint, biodegradable polymers are desirable, but they often have shorter service period due to decrease in mechanical strength caused by degradation and they are also more expensive than conventional petroleum-based polymers [8]. In recent years, researches have been devoted to prevent rapid degradation of biodegradable polymers during their shelf time as well as to obtain a new material with satisfactory price/performance ratio by blending biodegradable polymers and conventional petroleum-based polymers [9–11].

Polypropylene (PP), one of the popular petroleum-based polymers, possesses many merits such as highly availability, feasible processing, good stiffness, satisfactory heat resistance and low price. PP is widely used in automobile parts, commodity goods, textiles and electronic products [12–14]. Unlike the non-biodegradable PP [15], poly(lactic acid) (PLA) is a biodegradable polymer that is made from lactic acid produced via fermentation of carbohydrate crops such as corn, potato and sugar beet. PLA exhibits excellent performance such as biocompatibility, biodegradability, high stiffness and high strength, which leads to great potential in biomedical engineering and commodity applications [16–20]. Blending PP with PLA could obtain novel semi-

✉ Qiang Dou
douqiang.njut@163.com

¹ College of Materials Science and Engineering, Nanjing Tech University, Nanjing 210009, China

biocomposite with biodegradable property and acceptable price. In PP/PLA blends, the gradual decomposition of PP phase is induced by the removal of PLA phase by means of biodegradation, and this phenomenon is called biodisintegration [8, 21, 22].

The compatibility, morphology, rheological and mechanical properties of PP/PLA blends had been reported in the literature [5, 13, 15, 23, 24]. PP and PLA are immiscible because of the high polarity difference between them. Incorporation of compatibilizers such as maleic anhydride-grafted PP (MAH-g-PP), glycidyl methacrylate (GMA)-grafted polyethylene (GMA-g-PE) and ethylene-butyl acrylate-GMA terpolymer (E-BA-GMA) into the blends improved the compatibility and mechanical properties of the blends [5, 13, 23]. Kang et al. [13] observed the phase separation structures in PP/PLA blends. Hamad et al. [15] investigated the rheological properties of PP/PLA blends and found that the true viscosities of the blends were between those of the neat polymers, whereas the flow activation energies of the blends are less than those of the neat polymers. Moreover, Ebadi Dehaghani et al. [24] found that the crystallization behaviors of the blends had significant changes compared to the neat polymers.

The crystallization behaviors and kinetics of PP and PLA have been studied extensively [5, 14, 17, 24–28]. Carmen et al. [25] investigated the non-isothermal crystallization behaviors of PP and its talc-filled composites and found that talc induced an increase in PP crystallization rate. Some literature [5, 17, 24, 27, 28] reported that neat PLA crystallized difficultly during the cooling process and had no obvious exothermic peak on the DSC cooling curve, while the non-isothermal crystallization kinetics of the nucleated PLA samples could be investigated easily. However, less focus has been paid on the crystallization behaviors, especially the crystallization kinetics of PP/PLA blends, while the crystallization behaviors play important roles on physical and mechanical properties of the blends. Furthermore, the investigation on the crystallization kinetics of polymer blends is of academic significance because the second polymer in the blend may affect the crystallization property of the crystallizable primary component [29].

In this study, the non-isothermal crystallization kinetics of neat PP, PP/PLA (80/20) blend and PP/PLA/MAH-g-PP (64/20/16) blend were investigated by means of differential scanning calorimetry (DSC). The non-isothermal crystallization kinetics of the samples were analyzed by Jeziorny's and Mo's models. The nucleation parameters (K_g) and activation energies (ΔE) for non-isothermal crystallization were evaluated by the modified Lauritzen–Hoffman equation and Kissinger's method, respectively.

Experimental

Materials

PP [T30S, density: 0.91 g cm^{-3} , MFR = 3.0 g/10 min ($230 \text{ }^\circ\text{C}$ and 2.16 kg load), PetroChina Jingmen Petrochemical Co., Ltd., Jingmen, China], PLA [4032D, density: 1.25 g cm^{-3} , MFR = 7.5 g/10 min ($230 \text{ }^\circ\text{C}$ and 2.16 kg load), Nature Works, USA], MAH-g-PP [MAH = 0.3 mass\% , MFR = 50 g/10 min ($230 \text{ }^\circ\text{C}$ and 2.16 kg load), Nanjing Qiangren Plastics Co., Ltd., Nanjing, China] and industrial antioxidant (B215, Nanjing Hua Lim Chemical Co., Ltd., Nanjing, China) were commercially available.

Preparation of samples

PP, PLA and MAH-g-PP were dried at $80 \text{ }^\circ\text{C}$ under vacuum for 8 h before compounding. PP/PLA (80 mass%/20 mass%) blend and PP/PLA/MAH-g-PP (64 mass%/20 mass%/16 mass%) blends were prepared in an internal mixer (HL200, Jilin University Science & Technology Equipment Factory, Changchun, China) at the temperature of $200 \text{ }^\circ\text{C}$ and the rotor speed of 40 rpm. The blending time was 5 min. 0.2 mass\% B215 was added during the melt blending. The melt was cooled and cut into small pieces.

DSC analysis

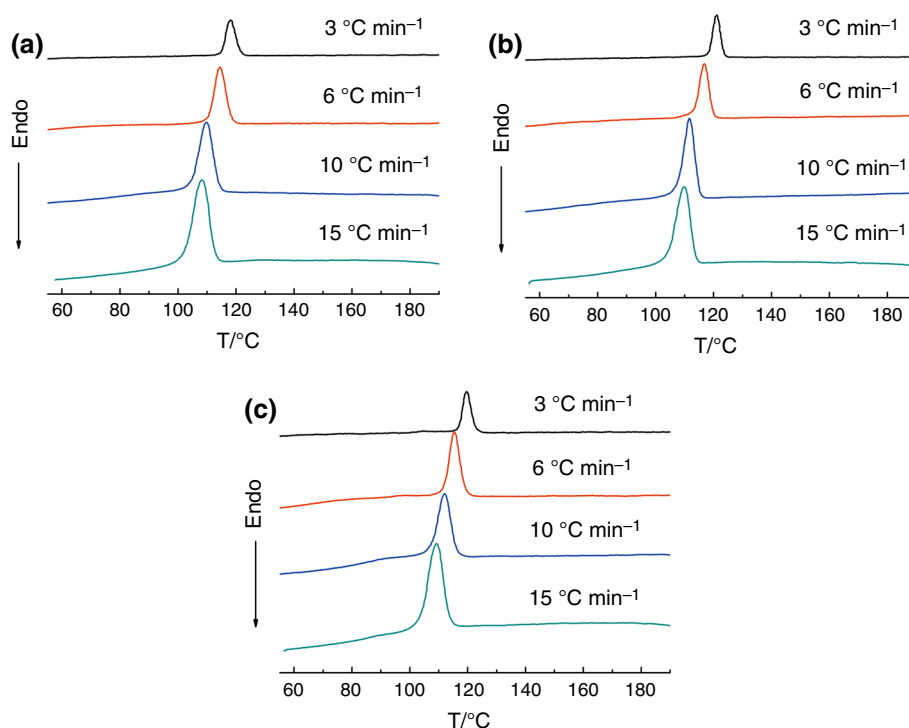
Non-isothermal crystallization experiments were performed using a DSC instrument (ZF-DSC-D2, Shanghai Zufa Industry Co., Ltd., Shanghai, China) under a dry nitrogen atmosphere. In each measurement, $\sim 4 \text{ mg}$ of sample was sealed in an aluminum pan. The sample was heated from room temperature to $210 \text{ }^\circ\text{C}$ at $10 \text{ }^\circ\text{C min}^{-1}$ and held at $210 \text{ }^\circ\text{C}$ for 5 min to eliminate the thermal history. Then, the melted sample was cooled to $50 \text{ }^\circ\text{C}$ at the constant cooling rate (Φ) of 3, 6, 10 and $15 \text{ }^\circ\text{C min}^{-1}$, respectively.

Results and discussion

Non-isothermal crystallization behaviors

The non-isothermal crystallization curves of neat PP, PP/PLA (80/20) blend and PP/PLA/MAH-g-PP (64/20/16) blend at different cooling rate (Φ) are shown in Fig. 1. Neat PLA crystallizes difficultly during the cooling process and had no obvious crystallization peak on the cooling curve [5, 17, 24, 27, 28]. Therefore, only the crystallization behaviors of PP phase in the blends were investigated. For each sample, the crystallization peak shifts to a lower

Fig. 1 Non-isothermal crystallization curves of samples. **a** Neat PP, **b** PP/PLA (80/20), **c** PP/PLA/MAH-g-PP (64/20/16)



temperature and becomes broader with the cooling rate. It is suggested that polymer chain movement is faster than the change of temperature at a low cooling rate, and thus, it takes a longer time to complete the crystallization, which leads to a higher temperature [30, 31].

The peak crystallization temperature (T_c^p) and the enthalpy of crystallization (ΔH_c) of the samples are listed in Table 1. It is widely believed that T_c^p and ΔH_c are related to the crystallization rate and represent the difficulty level of crystallization process. Generally, if a polymer has faster crystallization rate, it will crystallize at higher temperature [14, 27]. At the same cooling rate, the T_c^p of PP/PLA (80/20) blend is the biggest, implying that the crystallization rate of PP/PLA (80/20) blend is the fastest. The T_c^p of PP/PLA/MAH-g-PP (64/20/16) blend is slightly higher (0.6–1.6 °C) than that of neat PP. These minor temperature differences could not reveal the difference of crystallization rate between them convincingly. Therefore, the ΔH_c is introduced to denote the difficulty level of crystallization of the samples. The higher the ΔH_c value, the more perfect the

crystallization is. At the same cooling rate, the ΔH_c values of the samples are in the order: PP/PLA (80/20) blend > neat PP > PP/PLA/MAH-g-PP (64/20/16) blend. In PP/PLA (80/20) blend, the dispersed PLA particles may act as nucleating agents to make the crystallization of PP easier. However, the incorporation of MAH-g-PP may strengthen the phase interfaces between PP and PLA, and the crystallization of PP may be retarded by the “amorphous” PLA, and thus, PP/PLA/MAH-g-PP (64/20/16) blend shows a lower ΔH_c value than that of neat PP.

In the non-isothermal crystallization process, the relative crystallinity as a function of temperature, X_T , can be calculated according to Eq. (1):

$$X_T = \frac{\int_{T_0}^T (dH_c/dt)dT}{\int_{T_0}^{T_\infty} (dH_c/dt)dT} \tag{1}$$

where T_0 , T and T_∞ are the initial, arbitrary and final crystallization temperatures, respectively. Figure 2 shows X_T versus temperature curves of the samples. All curves

Table 1 T_c^p , $t_{1/2}$ and ΔH_c values for samples

$\Phi/^\circ\text{C min}^{-1}$	Neat PP			PP/PLA (80/20)			PP/PLA/MAH-g-PP (64/20/16)		
	$T_c^p/^\circ\text{C}$	$t_{1/2}/\text{min}$	$\Delta H_c/\text{J g}^{-1}$	$T_c^p/^\circ\text{C}$	$t_{1/2}/\text{min}$	$\Delta H_c/\text{J g}^{-1}$	$T_c^p/^\circ\text{C}$	$t_{1/2}/\text{min}$	$\Delta H_c/\text{J g}^{-1}$
3	118.1	2.12	101.2	121.1	1.66	107.8	119.7	2.26	95.5
6	114.6	1.18	92.1	116.8	0.88	94.1	115.4	1.28	90.7
10	109.8	0.79	85.6	111.6	0.63	89.6	110.4	0.79	83.3
15	108.2	0.55	72.3	109.9	0.44	76.3	109.2	0.56	70.8

exhibit reversed S-shape, indicating a fast primary process in the initial stage and a slower secondary process in the later stage. As the cooling rate decreases, the curves shift to higher temperature regions, indicating that the crystallization is strengthened as the temperature decreases, because the nucleation and crystallization processes are temperature-dependent [32]. The crystallization temperature during non-isothermal crystallization can be converted to the crystallization time:

$$t = \frac{T_0 - T}{\Phi} \quad (2)$$

Thus, the relative crystallinity (X_t) versus time curves can be obtained, as shown in Fig. 3. All curves exhibit S-shape. The crystallization half-time ($t_{1/2}$) is defined as the time at which the relative crystallinity is 50 % and can be directly determined from the curves, and the values are listed in Table 1. The shorter $t_{1/2}$, the faster the crystallization rate is. As expected, $t_{1/2}$ shortens with the cooling rate, indicating that a gradually accelerated crystallization rate as the cooling rate increases. Furthermore, at the same cooling rate, $t_{1/2}$ is in the order: PP/PLA/MAH-g-PP (64/20/16) blend > neat PP > PP/PLA (80/20) blend. This means that at the same cooling rate, the crystallization rate of PP in the PP/PLA (80/20) blend is the fastest and that in the PP/PLA/MAH-g-PP (64/20/16) blend is the slowest. For PP/PLA (80/20) blend, the dispersed PLA particles induce the heterogeneous nucleation of PP resulting in the highest crystallization rate. But the crystallization tendency of PP decreases in the presence of MAH-g-PP, which

relates to the decreased regularity of the chains due to the modification by maleic anhydride units [33]. For PP/PLA/MAH-g-PP (64/20/16) blend, the improved compatibility between PP and PLA by MAH-g-PP may weaken the nucleation effect of PLA because of the strengthened linkage between PP matrix and PLA phase. Moreover, the nucleating ability of a nucleating agent may be affected by many factors, for example, the crystal structure, surface topography and characteristics and grain size. The surface properties of PLA particles may be changed in PP/PLA/MAH-g-PP (64/20/16) blend. As a result, PP/PLA/MAH-g-PP (64/20/16) blend shows the slowest crystallization rate. The similar effects of the compatibilizers on the crystallization behaviors of the polymer blends were also reported in the literature. Liu et al. [34] reported that the addition of a compatibilizer (maleated thermoplastic elastomer, TPEg) weakened the nucleating role of PA6 in PP/PA6 blend. Yang et al. [35] found that the crystallization rate of PP in β -PP/PA6/MAH-g-PP blend was slower than that of uncompatibilized β -PP/PA6 blend.

Non-isothermal crystallization kinetics

Jeziorny's model

The classical Avrami's equation [36–38] is often employed to analyze the isothermal crystallization kinetics of a semicrystalline polymer, which can be expressed as follows:

Fig. 2 X_t versus temperature curves for samples. **a** Neat PP, **b** PP/PLA (80/20), **c** PP/PLA/MAH-g-PP (64/20/16)

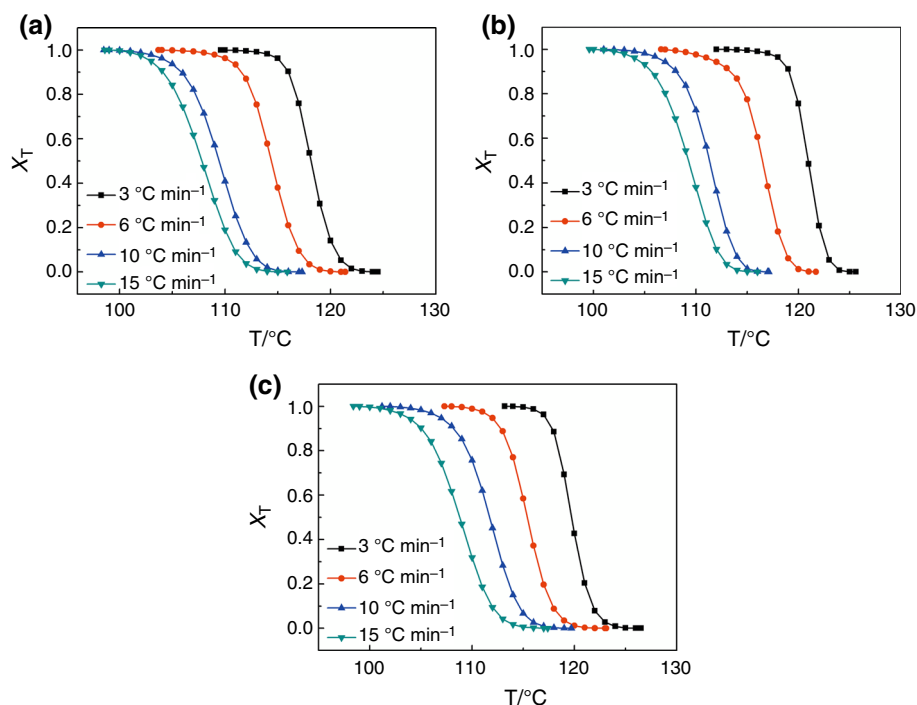
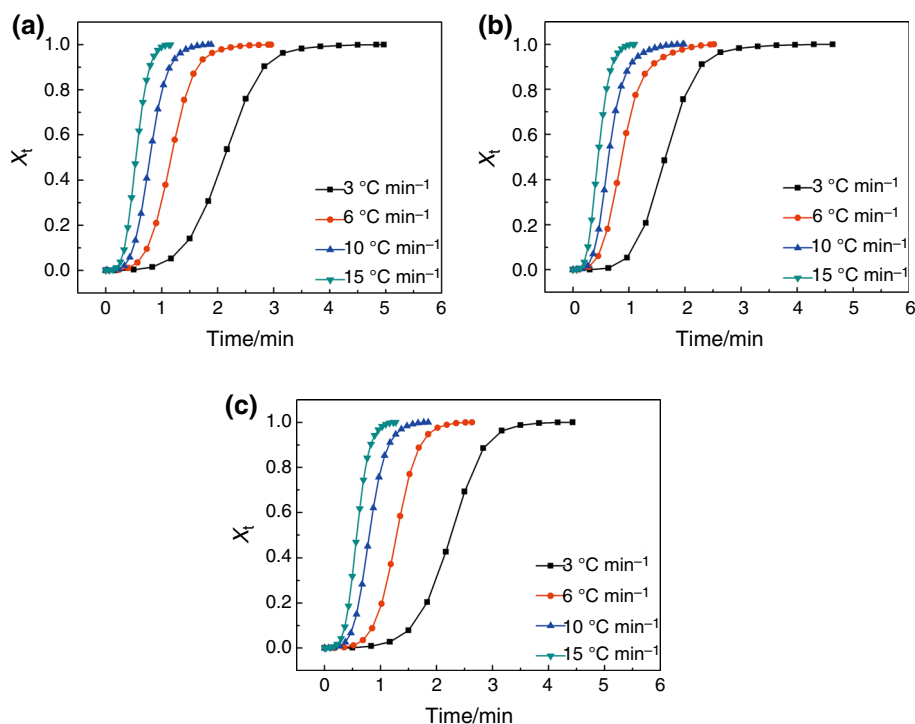


Fig. 3 X_t versus time curves for samples. **a** neat PP, **b** PP/PLA (80/20), **c** PP/PLA/MAH-g-PP (64/20/16)



$$1 - X_t = \exp(-Z_t t^n) \tag{3}$$

or

$$\lg[-\ln(1 - X_t)] = n \lg t + \lg Z_t \tag{4}$$

where X_t is the relative crystallinity at crystallization time t , n is the Avrami exponent, and Z_t is the crystallization rate constant involving both nucleation and growth rate parameters.

Jeziorny [39] modified Z_t in Avrami's equation with the cooling rate Φ to analyze the non-isothermal crystallization process:

$$\lg Z_c = \frac{\lg Z_t}{\Phi} \tag{5}$$

where Z_c is the modified crystallization rate constant, which is an independent rate constant. Figure 4 shows the plots of $\lg[-\ln(1 - X_t)]$ versus $\lg t$ of the samples, and Z_c , n and r^2 (linear correlation parameter) are listed in Table 2. According to r^2 value, the central parts of the curves ($X_t \approx 20\text{--}80\%$) show linear dependences. The deviation of the linear portion in the later stages is probably due to the secondary crystallization, and some initial dots are not considered because logarithmic plotting tends to overestimate small errors in the assessment of the initial crystallization time [14, 40]. For all samples, Z_c increases with the cooling rate, i.e., the crystallization rate accelerates with the supercooling. Furthermore, at the same cooling rate, Z_c is in the order: PP/PLA (80/20) blend > neat PP > PP/

PLA/MAH-g-PP (64/20/16) blend, which is in accordance with the $t_{1/2}$ results discussed above. The average n value of PP/PLA (80/20) blend is smaller than that of neat PP, indicating the heterogeneous nucleation effect of PLA on the crystallization of PP. But PP/PLA/MAH-g-PP (64/20/16) blend shows biggest average n value, suggesting that the PP phase tends to form more perfect spherulites in the presence of MAH-g-PP.

Mo's model

Ozawa [41] extended Avrami's equation by considering the influence of the cooling rate, and the relative degree of crystallization at temperature T , X_T , can be calculated as:

$$X_T = 1 - \exp\left(-\frac{K(T)}{\Phi^m}\right) \tag{6}$$

or

$$\lg[-\ln(1 - X_T)] = \lg K(T) - m \lg \Phi \tag{7}$$

where $K(T)$ is the cooling function, which relates to the overall crystallization rate and indicates how fast the crystallization proceeds, and m is the Ozawa exponent depending on the dimension of crystal growth.

In order to describe the non-isothermal crystallization process exactly, Liu et al. [42] proposed a new kinetic model by combining Avrami's and Ozawa's models, which is expressed as follows:

Fig. 4 $\lg[-\ln(1 - X_t)]$ versus $\lg t$ curves for the samples. **a** Neat PP, **b** PP/PLA (80/20), **c** PP/PLA/MAH-g-PP (64/20/16)

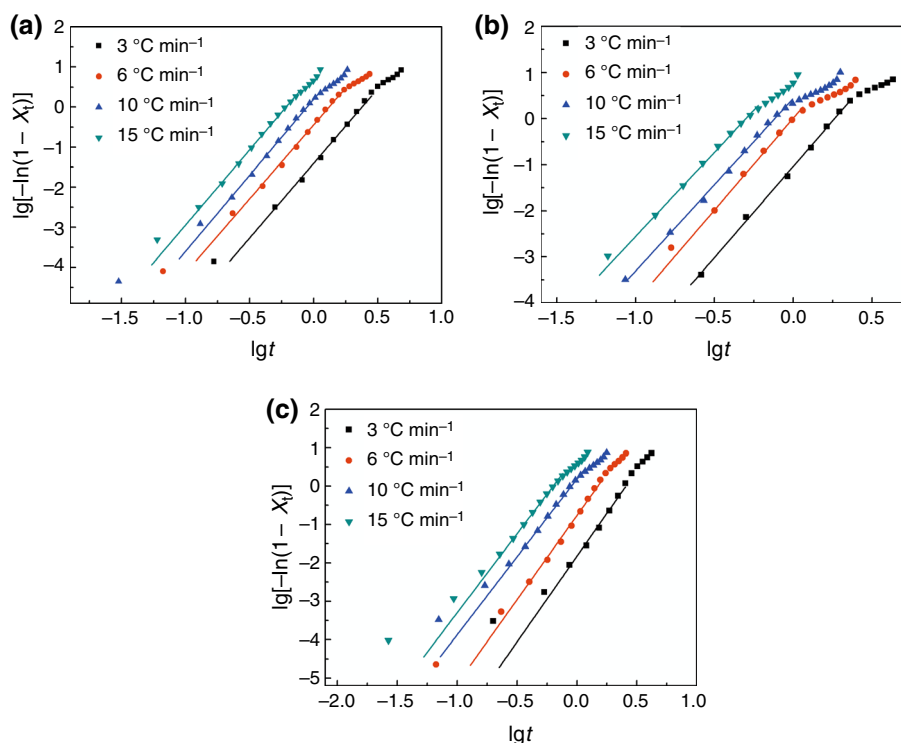


Table 2 Jeziorny's parameters for samples

Sample	$\Phi/^\circ\text{C min}^{-1}$	Z_c	n	Average n	r^2
Neat PP	3	0.33	4.29	3.93	0.998
	6	0.84	4.05		0.996
	10	1.04	3.76		0.998
	15	1.13	3.61		0.998
PP/PLA (80/20)	3	0.41	4.36	3.81	0.999
	6	1.00	3.89		0.999
	10	1.14	3.73		0.996
	15	1.18	3.27		0.998
PP/PLA/MAH-g-PP (64/20/16)	3	0.25	4.60	4.14	0.997
	6	0.78	4.25		0.997
	10	1.03	3.92		0.997
	15	1.12	3.81		0.999

$$\lg Z_c + n \lg t = \lg K(T) - m \lg \Phi \quad (8)$$

or

$$\lg \Phi = \lg F(T) - \alpha \lg t \quad (9)$$

where $F(T) = [K(T)/Z_c]^{1/m}$, when $\lg \Phi$ is plotted against $\lg t$, the intercept is $\lg F(T)$, and the slope is $-\alpha$. A higher $F(T)$ value means that a higher cooling rate is needed to reach a certain X_t in a unit of crystallization time, indicating a slow crystallization rate. $\alpha = n/m$, n is Avrami exponent, and m is Ozawa exponent.

Figure 5 shows the plots of $\lg \Phi$ versus $\lg t$ at different X_t of the samples, and $F(T)$, α and r^2 are listed in Table 3. According to r^2 value, all curves show good linear correlations, indicating that the experimental results can be described by Mo's method. For all samples, α values are greater than one, meaning that the Avrami exponent n is always greater than the Ozawa exponent m , and the similar results are found in the literature [43]. Moreover, α slightly increases with X_t . At the same X_t , α is in the order: PP/PLA (80/20) blend > neat PP > PP/PLA/MAH-g-PP (64/20/16)

blend. $F(T)$ systematically increases with X_t , suggesting that the cooling rate should be increased to obtain higher X_t in unit crystallization time. At the same X_t , $F(T)$ is in the order: PP/PLA/MAH-g-PP (64/20/16) blend > neat PP > PP/PLA (80/20) blend. This means that to reach the same X_t , the crystallization time required for PP/PLA (80/20) blend is the shortest and that for PP/PLA/MAH-g-PP (64/20/16) blend is the longest. This is also in accordance with the $t_{1/2}$ results.

Nucleation parameters for non-isothermal crystallization

The Lauritzen–Hoffman (L–H) equation is often used to describe the spherulite growth rate of isothermal crystallization [44]. The L–H equation is given as follows:

$$G = G_0 \exp\left[\frac{-U^*}{R(T_c^p - T_\infty)}\right] \exp\left[\frac{-K_g}{T_c^p(\Delta T)f}\right] \quad (10)$$

where G_0 is a pre-exponential term, U^* is the activation energy related to the short-distance diffusion of the crystalline unit across the phase boundary and is commonly given by a universal value of 6300 J mol^{-1} [45]. R is the universal gas constant. T_c^p is the peak crystallization temperature. T_∞ is the temperature below which there is no chain motion (usually $T_\infty = T_g - 30 \text{ K}$), ΔT is the degree of supercooling, $\Delta T = T_m^0 - T_c^p$, and T_m^0 is the equilibrium melting temperature (here T_m^0 is 485.3 K for iPP [46]). f is the corrective factor for variation of the enthalpy of fusion,

Table 3 Mo’s parameters for samples

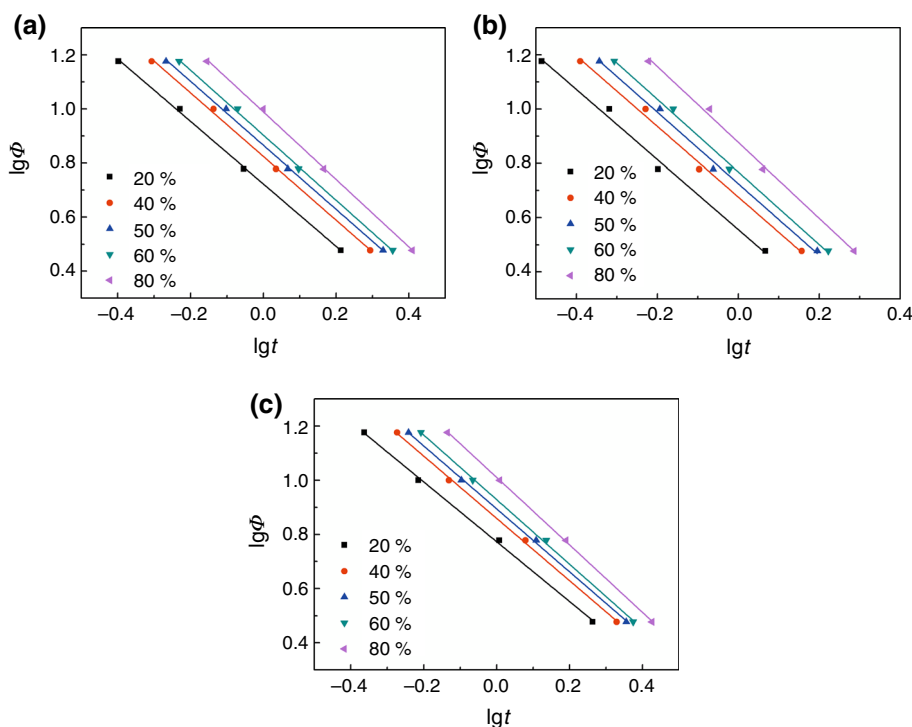
Sample	$X_t/\%$	F/T	α	r^2
Neat PP	20	5.28	1.15	0.999
	40	6.67	1.18	0.998
	50	7.34	1.19	0.998
	60	8.00	1.20	0.999
	80	9.75	1.25	0.999
PP/PLA (80/20)	20	3.60	1.29	0.987
	40	4.74	1.30	0.993
	50	5.30	1.32	0.993
	60	5.86	1.34	0.996
	80	7.53	1.40	0.995
PP/PLA/MAH-g-PP (64/20/16)	20	5.93	1.10	0.998
	40	7.23	1.15	0.996
	50	7.84	1.16	0.997
	60	8.48	1.19	0.998
	80	10.24	1.25	0.999

defined as $f = 2T_c^p / (T_m^0 + T_c^p)$, and K_g is the secondary nucleation parameter. The logarithmic transformation of Eq. (10) leads to:

$$\ln G + \frac{U^*}{R(T_c^p - T_\infty)} = \ln G_0 - \frac{K_g}{T_c^p(\Delta T)f} \quad (11)$$

Lim et al. [47] modified the L–H equation by substituting T_c^p with $(T_0 - \Phi)t$ to measure the spherulite growth rate as a function of temperature and cooling rate in non-

Fig. 5 $\lg\Phi$ versus $\lg t$ curves for samples. **a** Neat PP, **b** PP/PLA (80/20), **c** PP/PLA/MAH-g-PP (64/20/16)



isothermal crystallization and proposed the following equations:

$$\ln G + \frac{U^*}{R(T_0 - \Phi t - T_\infty)} = \ln G_0 - \frac{K_g}{(T_0 - \Phi t)[T_m^0 - (T_0 - \Phi t)]f} \quad (12)$$

$$f = \frac{2(T_0 - \Phi t)}{T_m^0 + (T_0 - \Phi t)} \quad (13)$$

G is the spherulite growth rate of non-isothermal crystallization, $G \approx (t_{1/2})^{-1}$ [48]. Nucleation parameter (K_g) can be determined from the slope of the plot of $\ln G + U^*/R(T_0 - \Phi t - T_\infty)$ versus $1/(T_0 - \Phi t)[T_m^0 - (T_0 - \Phi t)]f$ as shown in Fig. 6, and the results are listed in Table 4. The lower K_g value of PP/PLA (80/20) blend indicates that PLA particles act as effective nucleating agents for the crystallization of PP phase. Because the surface nucleation barrier is proportional to K_g , the decreased K_g value suggests PLA particles in the blend will result in the increased surface nucleation rate [49]. Huang [48] calculated the K_g values of neat PP and PP/CaCO₃ composites in the non-isothermal crystallization process and found that PP/CaCO₃ composites show a lower K_g value due to the nucleation effects of CaCO₃ particles on the crystallization of PP phase. However, the incorporation of MAH-g-PP restrains both the nucleation effects of PLA particles and the movement of PP chains, and thus, PP/PLA/MAH-g-PP (64/20/16) blend has the biggest K_g value.

Activation energy for non-isothermal crystallization

Considering the influence of different cooling rates in the non-isothermal crystallization process, Kissinger [50] proposed that the activation energy (ΔE) can be obtained by

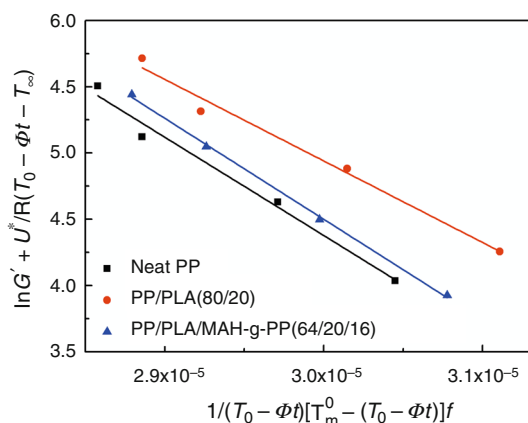


Fig. 6 $\ln G + U^*/R(T_0 - \Phi t - T_\infty)$ versus $1/(T_0 - \Phi t)[T_m^0 - (T_0 - \Phi t)]f$ curves for samples

Table 4 K_g and ΔE values for samples

Sample	$K_g/10^5 \text{ K}^2$	$\Delta E/\text{kJ mol}^{-1}$
Neat PP	7.42	194.7
PP/PLA (80/20)	6.16	176.1
PP/PLA/MAH-g-PP (64/20/16)	7.62	198.0

calculating the variation of the peak crystallization temperature with the cooling rate. Kissinger's method can be expressed as follows:

$$\frac{d\left[\ln\left(\frac{\Phi}{(T_c^p)^2}\right)\right]}{d(1/T_c^p)} = \frac{-\Delta E}{R} \quad (14)$$

or

$$\ln\left(\frac{\Phi}{(T_c^p)^2}\right) = \left(\frac{1}{T_c^p}\right)\left(\frac{-\Delta E}{R}\right) \quad (15)$$

where Φ is the cooling rate, T_c^p is the peak crystallization temperature (listed in Table 1), and R is the universal gas constant. ΔE can be determined from the slope of the plot of $\ln(\Phi/(T_c^p)^2)$ versus $1/T_c^p$ as shown in Fig. 7, and the results are listed in Table 4. PP/PLA (80/20) blend shows the lowest ΔE value, while PP/PLA/MAH-g-PP (64/20/16) blend shows the highest one, i.e., ΔE values are ranked as: PP/PLA (80/20) blend < neat PP < PP/PLA/MAH-g-PP (64/20/16) blend. From the viewpoint of activation energy, the lower ΔE value means the higher crystallization ability of the polymer system [18, 51]. PP/PLA (80/20) blend exhibits the lowest ΔE value, suggesting the dispersed PLA particles could make the crystallization of PP phase easier. PP/PLA/MAH-g-PP (64/20/16) blend exhibits the highest ΔE value due to the confinement effect of MAH-g-PP in the blend. It is well known that the crystallization process involves nucleation and crystal growth stages. The improved compatibility between PP and PLA by MAH-g-

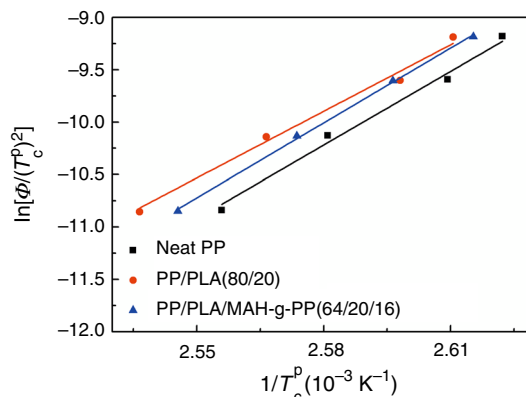


Fig. 7 $\ln[\Phi/(T_c^p)^2]$ versus $1/T_c^p$ curves for samples

PP weakens the nucleation effects of PLA particles. Furthermore, the addition of MAH-g-PP could restrict the folding of PP chains into the crystal surfaces. The double effects of MAH-g-PP make the crystallization of PP phase more difficult in the blend. These results could be verified by the above analysis.

Conclusions

In this paper, DSC was used to investigate the non-isothermal crystallization kinetics of neat PP, PP/PLA (80/20) and PP/PLA/MAH-g-PP (64/20/16) blends. The non-isothermal crystallization data were analyzed by Jeziorny's and Mo's models. The nucleation parameters (K_g) and activation energies (ΔE) of non-isothermal crystallization were calculated by the modified Lauritzen–Hoffman equation and Kissinger's method, respectively. The results show that, at the same cooling rate, the crystallization rate of the samples is in the order: PP/PLA (80/20) blend > neat PP > PP/PLA/MAH-g-PP. The non-isothermal crystallization kinetics of the samples can be appropriately described by Jeziorny's and Mo's models. It is also revealed that PP/PLA (80/20) blend has the fastest crystallization rate and PP/PLA/MAH-g-PP (64/20/16) blend has the slowest one. Moreover, K_g and ΔE values are in the order: PP/PLA/MAH-g-PP (64/20/16) blend > neat PP > PP/PLA (80/20) blend, and the results are consistent with those of crystallization kinetics analysis.

Acknowledgements This work was supported by the Innovation Foundation for Graduate Students of Jiangsu Province (KYLX15_0779) and the Priority Academic Program Development of Jiangsu Higher Education Institutions (PAPD).

References

- Anderson K, Schreck K, Hillmyer M. Toughening polylactide. *Polym Rev.* 2008;48(1):85–108.
- Arcana IM, Bundjali B, Yudistira I, Jariah B, Sukria L. Study on properties of polymer blends from polypropylene with polycaprolactone and their biodegradability. *Polym J.* 2007;39(12):1337–44.
- Hamad K, Kaseem M, Ko YG, Deri F. Biodegradable polymer blends and composites: an overview. *Polym Sci Ser A.* 2014;56(6):812–29.
- Jamshidian M, Tehrani EA, Imran M, Jacquot M, Desobry S. Poly-lactic acid: production, applications, nanocomposites, and release studies. *Compr Rev Food Sci Food Saf.* 2010;9(5):552–71.
- Choudhary P, Mohanty S, Nayak SK, Unnikrishnan L. Poly(L-lactide)/polypropylene blends: evaluation of mechanical, thermal, and morphological characteristics. *J Appl Polym Sci.* 2011;121(6):3223–37.
- Kim HS, Kim HJ. Miscibility and performance evaluation of natural-flour-filled PP/PBS and PP/PLA bio-composites. *Fiber Polym.* 2013;14(5):793–803.
- Lucas N, Bienaime C, Belloy C, Queneudec M, Silvestre F, Nava-Saucedo JE. Polymer biodegradation: mechanisms and estimation techniques. *Chemosphere.* 2008;73(4):429–42.
- Yoo TW, Yoon HG, Choi SJ, Kim MS, Kim YH, Kim WN. Effects of compatibilizers on the mechanical properties and interfacial tension of polypropylene and poly(lactic acid) blends. *Macromol Res.* 2010;18(6):583–8.
- Núñez K, Rosales C, Perera R, Villarreal N, Pastor JM. Poly(lactic acid)/low-density polyethylene blends and its nanocomposites based on sepiolite. *Polym Eng Sci.* 2012;52(5):988–1004.
- Reddy N, Nama D, Yang Y. Poly(lactic acid)/polypropylene polyblend fibers for better resistance to degradation. *Polym Degrad Stab.* 2008;93(1):233–41.
- Singh G, Kaur N, Bhunia H, Bajpai PK, Mandal UK. Degradation behaviors of linear low-density polyethylene and poly(L-lactic acid) blends. *J Appl Polym Sci.* 2012;124(3):1993–8.
- Bai H, Wang Y, Song B, Fan X, Zhou Z, Li Y. Nucleating agent induced impact fracture behavior change in PP/POE blend. *Polym Bull.* 2008;62(3):405–19.
- Kang HM, Lu X, Xu YS. Properties of immiscible and ethylene-butyl acrylate-glycidyl methacrylate terpolymer compatibilized poly(lactic acid) and polypropylene blends. *Polym Test.* 2015;43:173–81.
- Shi Y, Dou Q. Non-isothermal crystallization kinetics of β -nucleated isotactic polypropylene. *J Therm Anal Calorim.* 2013;112(2):901–11.
- Hamad K, Kaseem M, Deri F. Rheological and mechanical characterization of poly(lactic acid)/polypropylene polymer blends. *J Polym Res.* 2011;18(6):1799–806.
- Balakrishnan H, Hassan A, Wahit MU. Mechanical, thermal and morphological properties of poly(lactic acid)/linear low density polyethylene blends. *J Elastomers Plast.* 2010;42(3):223–39.
- Li C, Dou Q, Bai Z, Lu Q. Non-isothermal crystallization behaviors and spherulitic morphology of poly(lactic acid) nucleated by a novel nucleating agent. *J Therm Anal Calorim.* 2015;122(1):407–17.
- Shi N, Dou Q. Non-isothermal cold crystallization kinetics of poly(lactic acid)/poly(butylene adipate-co-terephthalate)/treated calcium carbonate composites. *J Therm Anal Calorim.* 2014;119(1):635–42.
- Tábi T, Suplicz A, Czigány T, Kovács JG. Thermal and mechanical analysis of injection moulded poly(lactic acid) filled with poly(ethylene glycol) and talc. *J Therm Anal Calorim.* 2014;118(3):1419–30.
- Tham WL, Poh BT, MohdIshak ZA, Chow WS. Thermal behaviors and mechanical properties of halloysite nanotube-reinforced poly(lactic acid) nanocomposites. *J Therm Anal Calorim.* 2014;118(3):1639–47.
- Sarasa J, Gracia JM, Javierre C. Study of the biodegradation of a bioplastic material waste. *Bioresour Technol.* 2009;100(15):3764–8.
- Yeh JT, Huang CY, Chai WL, Chen KN. Plasticized properties of poly(lactic acid) and triacetone blends. *J Appl Polym Sci.* 2009;112(5):2757–63.
- Lee HS, Kim JD. Effect of a hybrid compatibilizer on the mechanical properties and interfacial tension of a ternary blend with polypropylene, poly(lactic acid), and a toughening modifier. *Polym Compos.* 2012;33(7):1154–61.
- Ebadi-Dehaghani H, Barikani M, Khonakdar HA, Jafari SH. Microstructure and non-isothermal crystallization behavior of PP/PLA/clay hybrid nanocomposites. *J Therm Anal Calorim.* 2015;121(3):1321–32.
- Carmen A, José P, Miren I, Jeanette G, Carmen U. Characteristics of non-isothermal crystallization of polypropylene with and without talc. *e-Polymers.* 2004;4(1):298–313.

26. Shi N, Dou Q. Crystallization behavior, morphology, and mechanical properties of poly(lactic acid)/tributyl citrate/treated calcium carbonate composites. *Polym Compos.* 2014;35(8):1570–82.
27. Li C, Dou Q. Non-isothermal crystallization kinetics and spherulitic morphology of nucleated poly (lactic acid): effect of dilithium cis-4-cyclohexene-1,2-dicarboxylate as a novel and efficient nucleating agent. *Polym Adv Technol.* 2015;26(4):376–84.
28. Li C, Dou Q. Non-isothermal crystallization kinetics and spherulitic morphology of nucleated poly(lactic acid): effect of dilithium hexahydrophthalate as a novel nucleating agent. *Thermochim Acta.* 2014;594:31–8.
29. Chen H, Pyda M, Cebe P. Non-isothermal crystallization of PET/PLA blends. *Thermochim Acta.* 2009;492(1–2):61–6.
30. Di Lorenzo M, Silvestre C. Non-isothermal crystallization of polymers. *Prog Polym Sci.* 1999;24(6):917–50.
31. Nandi S, Ghosh AK. Crystallization kinetics of impact modified polypropylene. *J Polym Res.* 2007;14(5):387–96.
32. Seo Y, Kim J, Kim KU, Kim YC. Study of the crystallization behaviors of polypropylene and maleic anhydride grafted polypropylene. *Polymer.* 2000;41(7):2639–46.
33. Menyh ard A, Varga J. The effect of compatibilizers on the crystallisation, melting and polymorphic composition of β -nucleated isotactic polypropylene and polyamide 6 blends. *Eur Polym J.* 2006;42(12):3257–68.
34. Liu H, Xie T, Zhang Y, Ou Y, Yang G. Crystallization behaviors of polypropylene/polyamide-6 blends modified by a maleated thermoplastic elastomer. *Polym J.* 2006;38(1):21–30.
35. Yang Z, Zhang Z, Tao Y, Mai K. Effects of polyamide 6 on the crystallization and melting behavior of β -nucleated polypropylene. *Eur Polym J.* 2008;44(11):3754–63.
36. Avrami M. Kinetics of phase change. I General theory. *J Chem Phys.* 1939;7(12):1103–12.
37. Avrami M. Kinetics of phase change. II Transformation-time relations for random distribution of nuclei. *J Chem Phys.* 1940;8(2):212–24.
38. Avrami M. Granulation, phase change, and microstructure kinetics of phase change. III. *J Chem Phys.* 1941;9(2):177–84.
39. Jeziorny A. Parameters characterizing the kinetics of the non-isothermal crystallization of poly(ethylene terephthalate) determined by DSC. *Polymer.* 1978;19(10):1142–4.
40. Zeng A, Zheng Y, Qiu S, Guo Y. Isothermal crystallization and melting behavior of polypropylene with lanthanum complex of cyclodextrin derivative as a β -nucleating agent. *J Appl Polym Sci.* 2011;121(6):3651–61.
41. Ozawa T. Kinetics of non-isothermal crystallization. *Polymer.* 1971;12(3):150–8.
42. Liu T, Mo Z, Wang S, Zhang H. Nonisothermal melt and cold crystallization kinetics of poly(aryl ether ether ketone ketone). *Polym Eng Sci.* 1997;37(3):568–75.
43. Papageorgiou GZ, Achilias DS, Bikiaris DN, Karayannidis GP. Crystallization kinetics and nucleation activity of filler in polypropylene/surface-treated SiO₂ nanocomposites. *Thermochim Acta.* 2005;427(1–2):117–28.
44. Hoffman JD, Miller RL. Kinetic of crystallization from the melt and chain folding in polyethylene fractions revisited: theory and experiment. *Polymer.* 1997;38:3151–212.
45. Supaphol P, Spruiell JE. Thermal properties and isothermal crystallization of syndiotactic polypropylenes: differential scanning calorimetry and overall crystallization kinetics. *J Appl Polym Sci.* 2000;75(1):44–59.
46. Xu J, Srinivas S, Marand H, Agarwal P. Equilibrium melting temperature and undercooling dependence of the spherulitic growth rate of isotactic polypropylene. *Macromolecules.* 1998;31(23):8230–42.
47. Lim GBA, McGuire KS, Lloyd DR. Nonisothermal crystallization of isotactic polypropylene in dotriacontane. 2. Effects of dilution, cooling rate, and nucleating agent addition on growth rate. *Polym Eng Sci.* 1993;33(9):537–42.
48. Huang JW. Dispersion, crystallization kinetics, and parameters of Hoffman-Lauritzen theory of polypropylene and nanoscale calcium carbonate composite. *Polym Eng Sci.* 2009;49(9):1855–64.
49. Zhao S, Xin Z. Crystallization kinetics of isotactic polypropylene nucleated with organic dicarboxylic acid salts. *J Appl Polym Sci.* 2009;112(3):1471–80.
50. Kissinger HE. Variation of peak temperature with heating rate in differential thermal analysis. *J Res Natl Bur Stand.* 1956;57(4):217–21.
51. Fan Q, Duan F, Guo H, Wu T. Non-isothermal crystallization kinetics of polypropylene and hyperbranched polyester blends. *Chin J Chem Eng.* 2015;23(2):441–5.